THE ROYAL SOCIETY

Muon-spin-rotation studies of organic magnets

By S. J. Blundell

Department of Physics, University of Oxford, The Clarendon Laboratory, Parks Road, Oxford OX1 3PU, UK

A muon is an unstable spin-$\frac{1}{2}$ particle with a lifetime of 2.2 μs. Beams of spin-polarized positive muons can be prepared at accelerator facilities and then subsequently implanted in various types of condensed matter. Both the time and direction dependence of the subsequent positron emission can be monitored. This allows the precession and relaxation of the average muon-spin polarization to be measured and the local magnetic field in the sample to be directly inferred. The muon thus behaves essentially as a 'microscopic magnetometer' and is used to follow the magnetic order at a local level and to investigate both static and dynamic effects. This article outlines the principles of various experimental techniques that involve implanted muons, and reviews some recent experimental data on organic and molecular magnets.

Keywords: muon-spin rotation; organic magnets; molecular magnets; nitronyl nitroxides

1. Introduction

The technique of muon-spin rotation (μSR) is extremely useful for studying various magnetic and superconducting systems (for reviews of the technique, see Schenck (1985), Cox (1987), Dalmas de Réotier & Yaouanc (1997)). This is because the frequency of the spin precession of the implanted muon (as measured by the time dependence of the spatial asymmetry in the decay positron emission) is directly related to the magnetic field at the muon site; hence, the muon can be used as a 'microscopic magnetometer'. Muons have been found to be effective probes of various types of condensed-matter physics phenomena and their use has been aided by the development of a number of accelerator facilities, most notably TRIUMF (Vancouver), PSI (Villigen, near Zürich), ISIS (Rutherford Appleton Laboratory, Oxfordshire) and KEK (Tsukuba). The technique requires the use of bulk samples because the incident muons are formed with an energy of 4 MeV and penetrate a few hundred micrometres into any sample. Surface studies may be possible in the future with the development of 'slow muon' beams, in which the energy of the muon beam is reduced down to ∼1–10 eV. This is achieved either by moderation in thin layers of rare-gas solid (Morenzoni *et al.* 1994) or by resonant ionization of thermal muonium (μ^+e^- produced from the surface of a hot tungsten foil placed in a pulsed proton beam) by a pulsed laser source (Nagamine *et al.* 1995), although the efficiency of both of these processes is currently rather low.

μSR has been used extensively in the study of various organic materials (Blundell 1997), including conducting polymers (Hayes 1995; Pratt *et al.* 1997) and organic superconductors (Lee *et al.* 1997). The technique has its most obvious application in

Phil. Trans. R. Soc. Lond. A (1999) **357**, 2923–2937

the study of magnetic systems (Denison *et al*. 1979). As a general probe of magnetic materials it can be particularly useful because

(a) it is a *local* probe of internal fields;

(b) it can be used to follow an order parameter as a function of temperature;

(c) it works very well at millikelvin temperatures (the incident muons easily pass through the dilution refrigerator windows);

(d) it provides information on antiferromagnets, spin-gap systems and spin glasses as well as on ferromagnets;

(e) if there is a range of muon sites, it can provide information about internal magnetic-field distributions; and

(f) it provides information about magnetic fluctuations and spin dynamics, even above the magnetic transition temperature.

In this article, I will describe the technique and how it has been used to study various organic and molecular magnetic systems (for a review of organic and molecular magnetism, see Kahn (1993)).

2. Experimental techniques

At a number of locations in the world (see above), intense beams of muons are prepared artificially for research in condensed-matter physics. These are made by colliding a high-energy proton beam with a suitable target, which produces pions. The pions decay very quickly into muons; if one selects the muons arising from pions that have stopped in the target, the muon beam emerges completely spin polarized.

These muons can then be implanted into a sample but their energy is large, at least 4 MeV. Following implantation they lose energy very quickly (in 0.1–1 ns) to a few keV by ionization of atoms and scattering with electrons. A muon then begins to undergo a series of successive electron capture and loss reactions, which reduces the energy to a few hundred eV in *ca.* 1 ps. If muonium is ultimately formed, then electron capture ultimately wins and the last few eV are lost by inelastic collisions between the muonium atom and the host atoms. All of these effects are very fast so that the muon (or muonium) is thermalized very rapidly. Moreover, the effects are all Coulombic in origin and do not interact with the muon spin, so that the muon is thermalized in matter without appreciable depolarization. This is a crucial feature for muon-spin-rotation experiments. One may be concerned that the muon may only measure a region of sample that has been subjected to radiation damage by the energetic incoming muon. This does not appear to be a problem since there is a threshold energy for vacancy production, which means that only the initial part of the muon path suffers much damage. Beyond this point of damage, the muon still has sufficient energy to propagate through the sample a further distance, thought to be *ca.* 1 μm, leaving it well away from any induced vacancies (Chappert 1984).

The muon decays with a mean lifetime of 2.2 μs as follows:

$$\mu^+ \to e^+ + \nu_e + \bar{\nu}_\mu .$$

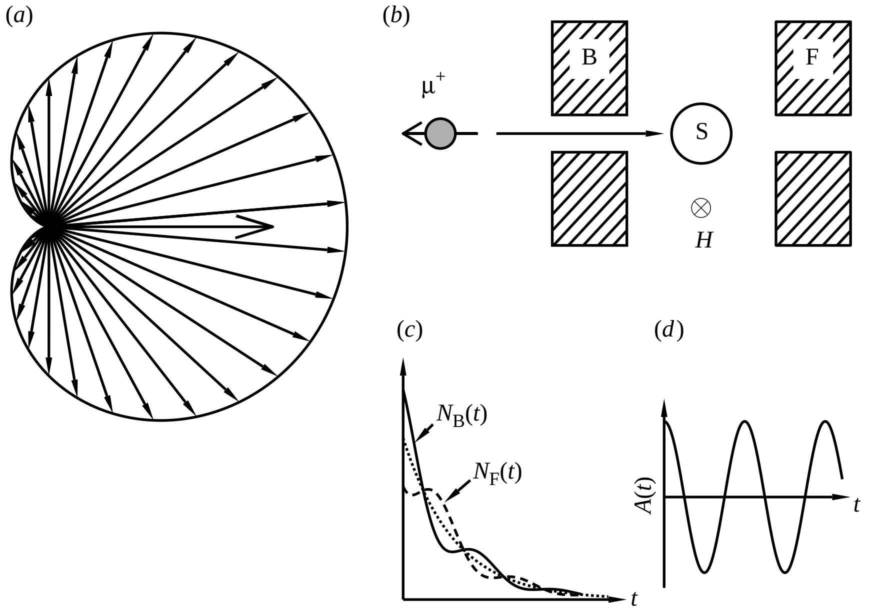

Figure 1. (*a*) The angular distribution of emitted positrons with respect to the initial muon-spin direction. The expected distribution for the most energetically emitted positrons is shown. (*b*) Schematic illustration of a μSR experiment. A spin-polarized beam of muons is implanted in a sample S. Following decay, positrons are detected in either a forward detector F or a backward detector B. If a transverse magnetic field H is applied to the sample as shown, then the muons will precess. (*c*) The number of positrons detected in the forward (dashed line) and backward (solid line) detectors. The dotted line shows the average of the two signals. (*d*) The asymmetry function.

The decay involves the weak interaction, which does not conserve parity, and this leads to a propensity for the emitted positron to emerge predominantly along the direction of the muon-spin when it decayed. The angular distribution of emitted positrons is shown in figure 1*a* for the case of the most energetically emitted positrons. In fact, positrons over a range of energies are emitted, so that the net effect is something not quite as pronounced, but the effect nevertheless allows one to follow the polarization of an ensemble of precessing muons with arbitrary accuracy, providing one is willing to take data for long enough.

A schematic diagram of the experiment is shown in figure 1*b*. A muon, with its polarization aligned antiparallel to its momentum, is implanted in a sample. (It is antiparallel because of the way that it was formed, see above, so the muon enters the sample with its spin pointing along the direction from which it came.) If the muon is unlucky enough to decay immediately, then it will not have time to precess, and a positron will be emitted preferentially into the backward detector. If it lives a little longer, it will have time to precess so that if it lives for half a revolution, the resultant positron will be preferentially emitted into the forward detector. Thus, the positron beam from an ensemble of precessing muons can be likened to the beam of light from a lighthouse.

The time evolution of the number of positrons detected in the forward and backward detector is described by the functions $N_{\mathrm{F}}(t)$ and $N_{\mathrm{B}}(t)$, respectively, and these are shown in figure 1*c*. Because the muon decay is a radioactive process, these two terms sum to an exponential decay. Thus the time evolution of the muon polarization can be obtained by examining the normalized difference of these two functions via the asymmetry function $A(t)$, given by

$$A(t) = \frac{N_{\mathrm{B}}(t) - N_{\mathrm{F}}(t)}{N_{\mathrm{B}}(t) + N_{\mathrm{F}}(t)}, \tag{2.1}$$

and is shown in figure 1*d*.

This experimentally obtained asymmetry function has a calculable maximum value, A_{max}, for a particular experimental configuration that depends on the initial beam polarization (usually very close to 1), the intrinsic asymmetry of the weak decay, and the efficiency of the detectors for positrons of different energies, and usually turns out to be $A_{\mathrm{max}} \sim 0.25$. The function can be normalized to 1, in which case it expresses the spin autocorrelation function of the muon, $G(t) = A(t)/A_{\mathrm{max}}$, which represents the time-dependent spin polarization of the ensemble of muons.

3. Experimental results

(*a*) *Nitronyl nitroxides*

Many organic radicals exist that have unpaired spins, but few are stable enough to be assembled into crystalline structures. Moreover, even when that is possible, *aligning* these spins ferromagnetically is usually impossible. Ferromagnets are rather rare, even among the elements, and are found exclusively in the d-block or f-block. Thus the discovery of ferromagnetism, albeit at rather low temperatures, in certain nitronyl nitroxide molecular crystals was particularly remarkable. The first material of this sort to be found was *p*-nitrophenyl nitronyl nitroxide (*p*-NPNN), which showed ferromagnetism up to $T_{\mathrm{C}} \sim 0.65$ K only in one of its crystal phases (Tamura *et al.* 1991; Kinoshita 1994). Nitronyl nitroxides contain only the elements C, H, N and O and are, therefore, fully organic. On each nitronyl nitroxide molecule there is an unpaired spin associated with the two N—O groups. Small chemical changes to the rest of the molecule lead to significant changes in crystal structure, thereby altering the intermolecular overlaps and, thus, the magnetic interactions between unpaired spins on neighbouring molecules. Thus, different compounds have greatly different magnetic ground states. Muon studies of this and related materials began soon after the initial discovery (Le *et al.* 1993*a*; Pratt *et al.* 1993; Blundell *et al.* 1994, 1995, 1996).

Following muon implantation, it is thought that muonium (Mu = μ^+e^-), with a single electronic spin, attaches to a particular nitronyl nitroxide and combines with the unpaired spin on the nitronyl nitroxide. As shown in figure 2, the resulting electronic spin state of the muonated radical may be a singlet ($S = 0$, leading to a diamagnetic state) or a triplet ($S = 1$, leading to a paramagnetic state; see Blundell *et al.* (1995)). Both states are found in experiments. In a diamagnetic state, the muon-spin precesses at a frequency $\nu_\mu = \gamma_\mu B = 0.1355\ \mathrm{MHz\ mT^{-1}} \times B$, so the frequency of the precession signal directly yields the local field B at the muon site. (γ_μ is the muon gyromagnetic ratio.) In a paramagnetic state, the muon-spin precesses at very

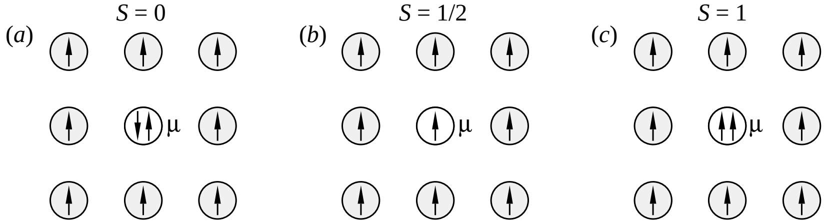

Figure 2. Electronic spin states following muon implantation in a nitronyl nitroxide system. In each case, the (*a*) singlet, (*b*) doublet and (*c*) triplet states are surrounded by nearest neighbours each with an unpaired spin. (*a*) and (*c*) are formed by Mu $= \mu^+e^-$ addition. (*b*) is formed by μ^+ addition. The muon-spin is not shown in each case (after Blundell *et al.* 1995).

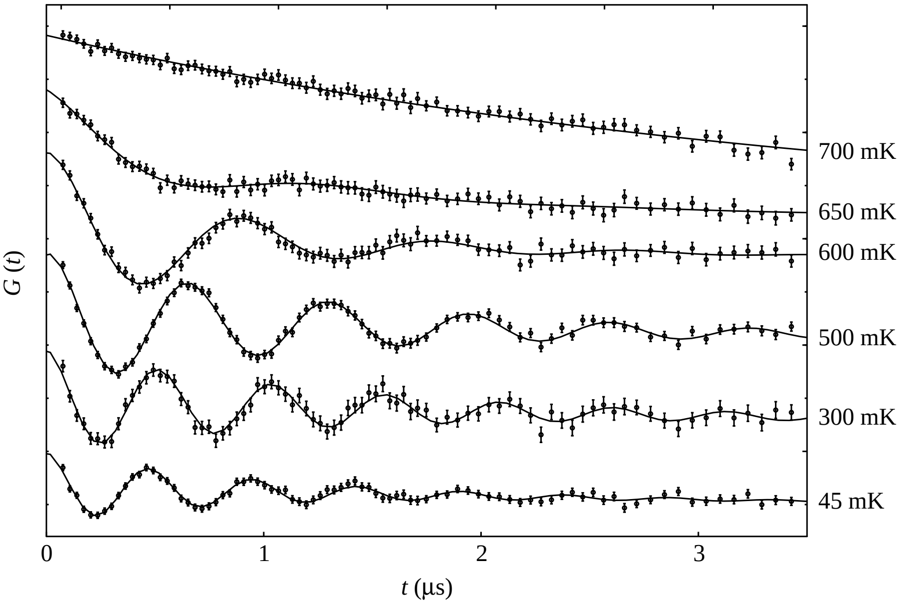

Figure 3. Zero-field muon-spin-rotation frequency in the organic ferromagnet *p*-NPNN (Blundell *et al.* 1995). The data for different temperatures are offset vertically for clarity.

high frequency in the hyperfine field, and the presence of this state can be detected via a loss of muon polarization at $t = 0$.

In figure 3, the time evolution of the muon polarization in polycrystalline *p*-NPNN is plotted as a function of temperature (Blundell *et al.* 1995). This is an example of an experiment with zero applied magnetic field (in fact, a small magnetic field was applied to compensate the effect of the Earth's field). At *ca.* 0.67 K there is a clear change between the high-temperature paramagnetic state, in which there are no oscillations, and the low-temperature ordered state, in which clear oscillations can be seen. As the sample is warmed, the frequency of oscillations decreases as the internal field decreases until it is above the Curie temperature and no oscillations can be observed, only a weak spin relaxation arising from spin fluctuations. The temperature dependence of the precession frequency ($\nu_\mu(T)$) of these oscillations is shown in figure 4 together with the calculated local internal field. This is fitted

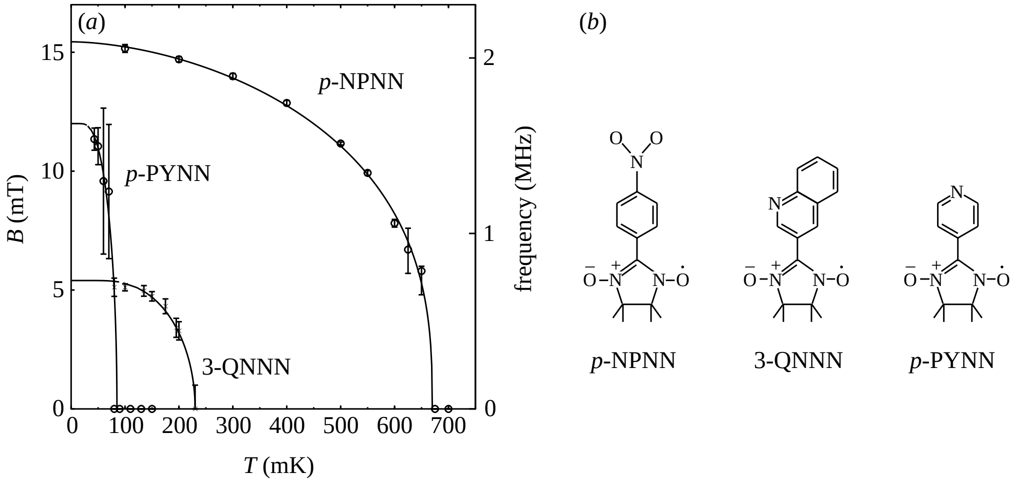

Figure 4. Temperature dependence of the zero-field muon-spin-rotation frequency in p-NPNN, 3-QNNN and p-PYNN (Blundell *et al*. 1994, 1995, 1997*b*). The fitted curve for p-NPNN is as described in the text. For 3-QNNN and p-PYNN, the fitted curve assumes a mean-field dependence. The molecular structure of each compound is also shown.

to a functional form $\nu_\mu(T) = (1 - (T/T_C)^\alpha)^\beta$, yielding $\alpha = 1.7 \pm 0.4$ and $\beta = 0.36 \pm 0.05$. This is consistent with three-dimensional long-range magnetic order. Near T_C, the critical exponent is as expected for a three-dimensional Heisenberg model (one expects $\beta \approx 0.36$ in this case). At low temperatures, the reduction in local field is consistent with a Bloch-$T^{3/2}$ law, indicative of three-dimensional spin waves (Blundell *et al*. 1995).

For p-NPNN, the magnetic properties were first determined using conventional magnetic measurements (Tamura *et al*. 1991). However, the ease of combining μSR with very low temperatures has led to ordered states being discovered using muons. In 3-quinolyl nitronyl nitroxide (3-QNNN), μSR oscillations have been observed below 210 mK and a lower local field at the muon site. The reduced local field is consistent with a canted magnetic structure (Pratt *et al*. 1993; Blundell *et al*. 1997*b*). The crystal structure of p-pyridyl nitronyl nitroxide (p-PYNN) is very different and consists of one-dimensional chains in which molecules are arranged side-by-side and head-to-tail (Blundell *et al*. 1994). This favours ferromagnetic interactions along the chain, but the inter-chain interactions are thought to be antiferromagnetic. Weak μSR oscillations below ∼90 mK are observed superimposed on a large background (Blundell *et al*. 1994), reflecting this more complicated magnetic structure. The temperature dependence of the precession frequencies of these three compounds, together with their molecular structures, is shown in figure 4.

The dependence of the magnetic ground state on the molecular shape is well illustrated by the chemical isomers 1-NAPNN and 2-NAPNN (NAPNN is naphthyl nitronyl nitroxide), whose different molecular shapes lead to different crystal packing and, consequently, different magnetic properties, and, hence, μSR behaviour (Blundell *et al*. 1996) (1-NAPNN shows a magnetic transition, 2-NAPNN does not). For the isomers 2-HOPNN and 4-HOPNN (HOPNN is hydroxy-phenyl nitronyl nitroxide), the former gives oscillatory μSR data which are characteristic of three-dimensional ordering below *ca.* 0.5 K, but the latter shows only low-frequency oscillations below *ca.* 0.7 K with evidence of a dimensional magnetic crossover at 0.1 K (Garçia-Muñoz *et al.* 1998). A magnetic transition has also been found in *p*-CNPNN (CNPNN is cyanophenyl nitronyl nitroxide, see Blundell *et al.* (1997*a*)). The overlaps in all these materials that favour ferromagnetism appear to agree with the McConnell mechanism: as a result of spin polarization effects, positive and negative spin density may exist on different parts of each molecule; intermolecular exchange interactions tend to be antiferromagnetic, so, if the dominant overlaps are between positive (majority) spin density on one molecule and negative (minority) spin density on another molecule, the overall intermolecular interaction may be ferromagnetic. Though the mechanism for ferromagnetism is electronic, the low values of T_C imply that the dipolar interactions will play an additional role in contributing to the precise value of T_C and determining the easy magnetization axis. This too depends on the crystal structure, which in turn depends on the molecular shape (Sugano *et al.* 1997).

(*b*) *Other organic magnetic materials*

An early candidate for organic ferromagnetism was the galvinoxyl radical, in which an unpaired electron is shared between the two symmetrically related halves of the molecule. Magnetic measurements revealed rather large intermolecular ferromagnetic interactions in the temperature range 85–300 K (Mukai *et al.* 1967). The magnetic susceptibility increased much faster than expected for isolated radicals as the temperature was decreased. The data give a Curie–Weiss constant of +11 K, which corresponds to $J \sim 10\,\mathrm{cm}^{-1}$, assuming that galvinoxyl behaves magnetically as a linear chain of spins. However, at 85 K an abrupt phase transition occurs and most of the paramagnetism vanishes. It is thought that this phase transition is accompanied by a dimerization of the galvinoxyl units, affording antiferromagnetically coupled pairs. This interpretation is supported by the fact that at 77 K the EPR spectrum shows a fine structure characteristic of a triplet state (Mukai *et al.* 1982). The intermolecular interaction between adjacent units is, therefore, ferromagnetic above 85 K and antiferromagnetic below 85 K. µSR data show Gaussian relaxation across the entire temperature range and no precession signal. This is indicative of the fact that there is no transition to long-range magnetic order.

Tanol suberate is a biradical with formula $(C_{13}H_{23}O_2NO)_2$. The susceptibility follows a Curie–Weiss law with a positive Curie temperature (+0.7 K). The specific heat exhibits a λ anomaly (Saint Paul & Veyret 1973) at 0.38 K and is found to be an antiferromagnet, but, in a field of 6 mT, it undergoes a metamagnetic transition (Benoit *et al.* 1985; Chouteau & Veyret-Jeandey 1981). µSR experiments yield clear spin precession oscillations (Sugano *et al.* 1999). The temperature dependence of the precession frequency follows the equation $\nu_\mu(T) = \nu_\mu(0)(1-T/T_C)^\beta$, where $\beta = 0.22$. This critical exponent is consistent with a two-dimensional XY magnet (Bramwell & Holdsworth 1993) and also with the temperature dependence of the magnetic susceptibility (Sugano *et al.* 1999). The relaxation rate of the oscillations rises to a maximum at the transition temperature and then falls dramatically, as shown in figure 5.

A variety of other organic magnetic materials exist and have been studied using µSR, but the nitronyl nitroxides remain the main source of purely organic bulk ferromagnets to date (recently, magnets based on TEMPO radicals have been discovered

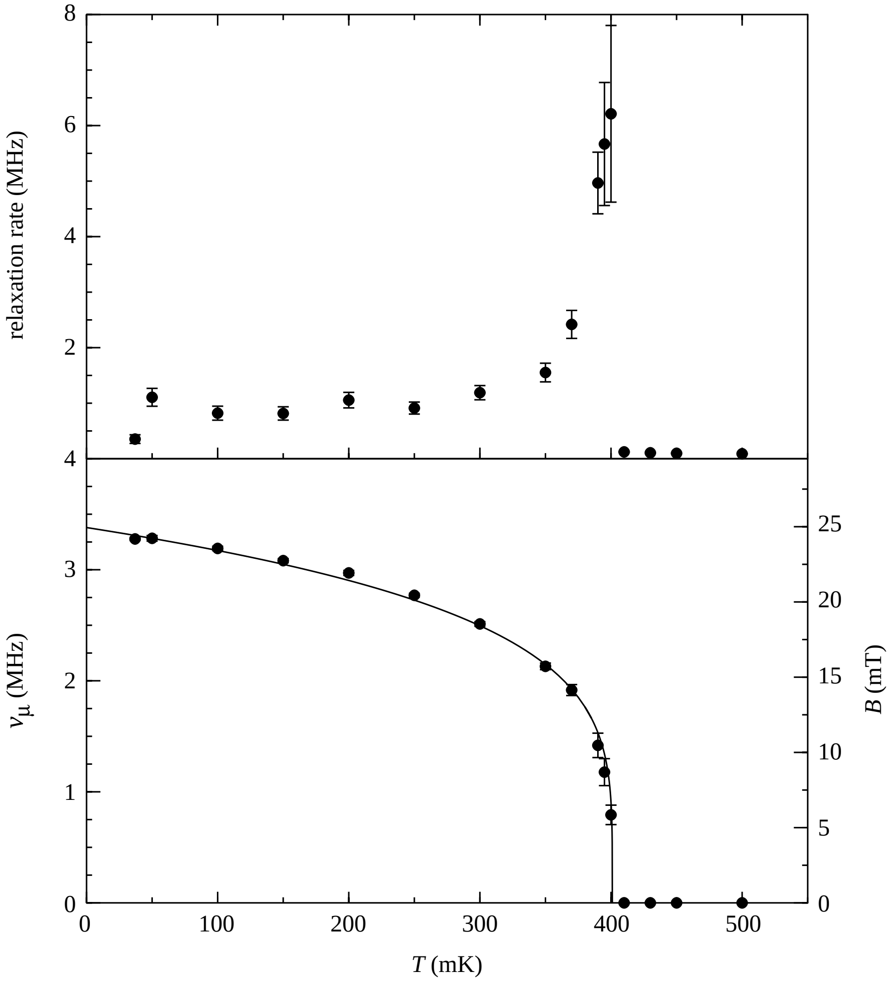

Figure 5. μSR data measured on tanol suberate showing the temperature dependence of the relaxation rate and frequency of the muon-spin oscillations.

and a μSR study has been reported (Imachi *et al.* 1997)). Another initially promising candidate was prepared by using the organic donor TDAE to make a charge-transfer salt with C_{60} (Allemand *et al.* 1991). The resulting material, TDAE-C_{60}, is electrically conducting and shows a ferromagnetic-like transition at 16.1 K. However, this is not metallic and a μSR experiment (Lappas *et al.* 1995) shows a broad distribution of internal fields at the muon site, which could be consistent with incommensurate magnetic order resulting from density-wave formation.

Some of the most technologically promising materials are molecular magnets in which a transition metal ion provides the localized moment and organic bridges act as exchange pathways. Progress has been achieved using materials with unpaired electrons on both the metal ions and on the organic molecules, as in (DMeFc)TCNE (Chittipeddi *et al.* 1987) (where DMeFc=$[Fe((CH_3)_5C_5)_2]$ is a donor and TCNE is an acceptor). This material has a chain structure but shows bulk ferromagnetic order below 4.8 K. Muons have been used to measure the development of short-range spin correlations above this temperature, which are very slow in this quasi-one-dimensional material (Uemura *et al*. 1994). Molecular magnets can also be made using the dicyanamide ligand; in particular, $\mathrm{Ni(N(CN)_2)_2}$ and $\mathrm{Co(N(CN)_2)_2}$ have been prepared and show long-range ferromagnetic order below 21 K and 9 K, respectively (Kurmoo & Kepert 1998). μSR experiments on these materials detect the magnetic order by a loss of muon polarization below T_C but have not been able to resolve a precession signal, suggesting a broad internal field distribution. Significant spin relaxation is observed in the paramagnetic state, which persists well above T_C.

μSR can also be useful for studying gapped systems. One such organic example is $\mathrm{MEM(TCNQ)_2}$, which undergoes a spin-Peierls (SP) transition at low temperature. This is an intrinsic lattice instability in spin-$\frac{1}{2}$ antiferromagnetic Heisenberg chains. Above the transition temperature T_SP, there is a uniform antiferromagnetic next-neighbour exchange in each chain; below T_SP, there is an elastic distortion resulting in dimerization, and, hence, two unequal alternating exchange constants. The alternating chain possesses an energy gap between the singlet ground state and the lowest lying band of triplet excited states that closes up above T_SP. μSR studies indicate a slowing down of the electronic fluctuations resulting from the opening of a gap in the magnetic excitation spectrum as the temperature is lowered below T_SP (Blundell *et al*. 1997*c*; Lovett *et al*. 1999).

(*c*) *Charge-transfer salts*

Various charge-transfer salts of the organic molecules TMTSF and BEDT-TTF are found to be very good metals. The properties of these salts can be tuned by small variations of the anion (for example, $\mathrm{(BEDT\text{-}TTF)_2NH_4Hg(SCN)_4}$ is a superconductor with $T_\mathrm{C} = 1$ K, while the isostructural $\mathrm{(BEDT\text{-}TTF)_2KHg(SCN)_4}$ is not). In a number of these metallic charge-transfer salts it is found that there is a competition between a spin-density wave (SDW) ground state and a superconducting ground state. Thus the SDW state is of great interest to study, since its presence precludes superconductivity. If the muon occupies one site per unit cell and the SDW is commensurate with the crystal lattice, a number of distinct muon-spin precession frequencies would be expected to be measured. If the SDW is incommensurate, a Bessel function relaxation (Le *et al*. 1993*b*) is predicted if the field at the muon site varies sinusoidally, easily recognized since the maxima and minima appear shifted by a $\pi/4$ phase. The SDW state in $\mathrm{(TMTSF)_2X}$, where $\mathrm{X{=}PF_6}$, $\mathrm{NO_3}$ or $\mathrm{ClO_4}$, has been detected using μSR with similar amplitude for all three compounds (Le *et al*. 1993*b*). The observed oscillations are consistent with an incommensurate SDW. In $\mathrm{(BEDT\text{-}TTF)_2KHg(SCN)_4}$ a very weak SDW (of estimated amplitude $3\times10^{-3}\mu_\mathrm{B}$) has been detected (Pratt *et al*. 1995) below 12 K. Too small to be seen by NMR, this SDW state was suspected on the basis of susceptibility and Fermi surface experiments, but appeared in μSR data as a small change in zero-field spin relaxation.

4. Dipole fields

In many magnetic systems the implanted muon is located at a *unique* crystallographic site, so that the muon-spin precession frequency can be used to deduce directly the magnetic field at that site (which is similarly unique, neglecting any time-dependent fluctuating fields). In more complicated cases, muons may occupy more than one crystallographically independent site, leading to more than one muon-spin precession frequency. In both cases the temperature dependence of these frequencies measured in zero applied field can be used to follow the order parameter (Denison *et al*. 1979).

This situation can be contrasted with that of type II superconducting systems in an applied field. Here it is immaterial whether the muon stops in a unique crystallographic site. The magnetic field at the muon site depends mainly on its position with respect to the (much larger) vortex lattice. The vortex lattice is usually incommensurate with the crystallographic lattice. In these experiments an ensemble of muons measures the *field distribution* $p(B)$, which is, in effect, the probability of measuring a field B for a muon placed 'at random'. The detailed form of $p(B)$ can yield the penetration depth (Brandt 1988; Seeger & Brandt 1986) and also information concerning vortex lattice melting (Lee *et al*. 1997).

In very complex organic systems one may have something of an intermediate situation. One does not expect to observe a single muon precession frequency, but, rather, a large (perhaps very large) number of different frequencies, which reflects the large distribution of muon sites in the unit cell. Therefore, it may be fruitful to approximate this situation by the convenient fiction that the muon occupies *all* possible positions in the unit cell. Thus one is concerned with a magnetic-field distribution (as in the case of experiments on type II superconductors) that arises from the dipolar fields from a lattice of magnetic moments.

The magnetic field $\boldsymbol{B}(\boldsymbol{r})$ at position $\boldsymbol{r}$ in the unit cell is given by

$$\boldsymbol{B}(\boldsymbol{r}) = \frac{\mu_0}{4\pi} \sum_i \frac{3(\boldsymbol{m}_i \cdot \hat{\boldsymbol{R}}_i)\hat{\boldsymbol{R}}_i - \boldsymbol{m}_i}{R_i^3}, \tag{4.1}$$

where $\boldsymbol{R}_i = \boldsymbol{r} - \boldsymbol{r}_i$, $R_i = |\boldsymbol{R}_i|$, $\hat{\boldsymbol{R}}_i = \boldsymbol{R}_i/R_i$, and the sum runs over all magnetic moments $\boldsymbol{m}_i$ at sites $\boldsymbol{r}_i$. The sum is taken over the infinite lattice, but it is well known that this sum converges in such a way that it is necessary only to sum over points inside a sphere centred on $\boldsymbol{r}$ with sufficiently large radius. Calculations of dipole fields using this method have been performed for some time (McKeehan 1933). (An alternative method of calculation is provided by Ewald; for details see Bowden & Clark (1981)). For a spherical sample this calculation would yield the correct local field, but for other shapes the Lorentz field, $\mu_0\boldsymbol{M}/3$, and the demagnetizing field, must be considered, though for spherical samples these two terms cancel. For an antiferromagnetic lattice of spins, these two terms do not contribute. I will ignore these corrections below since they change only the details, rather than the main features, of the field distribution in each case. In what follows, we will be concerned with the distribution of the magnitude of the field $|\boldsymbol{B}(\boldsymbol{r})|$, since in polycrystalline samples this is the quantity that is directly relevant to μSR.

As an example, consider a cubic unit cell of side 10 Å with $1\mu_{\mathrm{B}}$ moments on each corner (this is typical for a real organic system, although many real examples may be more magnetically dilute). All moments in the lattice are aligned as shown. Figure 6*a* shows the unit cell of this example, and contours of the field distribution $B = |\boldsymbol{B}|$ are drawn on each face of the cube. Close to each corner (say a distance d away) the local field is dominated by the corner moment and grows as d^{-3}. Near each corner the contours are, therefore, not shown. The corresponding field distribution $p(B)$ is plotted in figure 6*b*. The high-field tail of this distribution falls as B^{-2} and

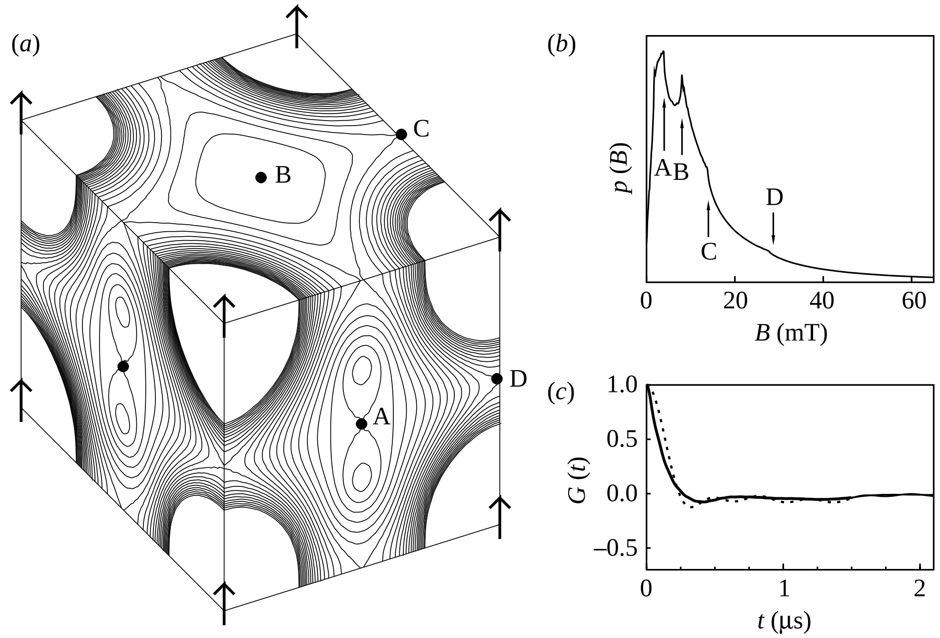

Figure 6. A simple cubic lattice of ferromagnetically aligned magnetic moments. (*a*) Contours of $|\boldsymbol{B}|$ are shown on the faces of the cubic unit cell. (Moments shown as vertical arrows.) (*b*) Field distribution $p(B)$. The singularities marked correspond to the points marked in (*a*). (*c*) Corresponding muon relaxation function $G(t)$ (solid line). The dotted line shows the result when only considering sites with $B < 20$ mT.

corresponds to the regions near each corner. The asymmetric lineshape is typical of these types of dipolar lattice. In addition, various discontinuities can be seen (four of them are labelled A, B, C and D), and these correspond to van Hove singularities in the field distribution. (They correspond to the four points marked A, B, C and D in figure 6*a*.) If we assume that muons find static sites in this lattice completely at random, then they will show a precession frequency distribution that exactly follows the field distribution. The corresponding muon relaxation function,

$$G(t) = \int_0^\infty \mathrm{d}B\, p(B) \cos(\gamma_\mu B t) \Big/ \int_0^\infty \mathrm{d}B\, p(B),$$

is shown by the solid line in figure 6*c*. It is characterized by a fast initial decay followed by a very weakly oscillating plateau.

In a real material, the ensemble of muons would not, of course, occupy *every* position in the unit cell, but would select a small subset of points, chosen roughly ‘at random’ from the $p(B)$ probability distribution. (The choice is, of course, governed by electrostatic considerations (Valladares *et al.* 1998), but is, in general, uncorrelated with the magnetic-field distribution.) However, we should ignore muons that stop very close to the electronic moments at the corners since this leads to the formation of paramagnetic states (Blundell *et al.* 1995). In order to gain some qualitative understanding of this effect, one should examine the dotted line in figure 6*c*, which shows $G(t)$ calculated from $p(B)$ but excludes any muon-site with a local field larger than 20 mT (i.e. cutting off $p(B)$ above 20 mT). This truncation produces weak oscillations in the relaxation function. The asymmetric $p(B)$ lineshape produces a fast initial relaxation followed by very weak oscillations in the calculated muon relaxation function $G(t)$. This feature is likely to be robust even if the muon samples only a few points ('at random') from the $p(B)$ distribution, except, of course, that the oscillations in $G(t)$ will be much stronger.

This fast initial relaxation behaviour is rather reminiscent of that observed in a number of experiments on organic magnetic materials, in particular the organic nitronyl nitroxides p-PYNN and 1-NAPNN (Sugano *et al*. 1995, 1997; Blundell *et al*. 1994, 1996). In the former case, weak oscillations were observed below the magnetic transition temperature T_C superimposed upon a fast relaxation (Blundell *et al*. 1994); in the latter case, no oscillations were observed, but the magnetic transition temperature was inferred by the development of a fast relaxation (Blundell *et al*. 1996). It was not clear from these experiments whether this fast relaxation could be ascribed to a static or dynamic effect; the present work provides some rationale for interpreting the fast relaxation as a purely static effect. Moreover, μSR experiments are currently being attempted on more chemically complex magnetic materials, in which there is a likelihood of many muon stopping sites in the unit cell; it may therefore be possible to use methods akin to those outlined above to interpret the results, because in such a regime it is appropriate to consider field *distributions.* It has been assumed throughout that the magnetic moments are point dipoles; if, instead, they have some small spatial distribution, this will have most effect on the high-field tail of the $p(B)$ distribution, rather than on the shape of the lower-field part. In addition, the extension to non-cubic lattices is straightforward.

Of course, in many organic systems a single precession frequency can be observed (e.g. in p-NPNN and tanol suberate described in § 3), but the analysis presented above is likely to be relevant in systems of increasing complexity.

5. Conclusions

Muon-spin rotation has recently been attempted on complex organic systems that show a variety of types of magnetic order. It is clear from these studies that μSR has a lot to offer by providing magnetic information from a purely local level. Experiments can be performed on powder or single-crystal samples over a large range of temperatures. The precession frequencies are typically low in comparison with inorganic systems because the magnetic moments are less dense. This makes the experiments easy to perform at muon facilities with low precession frequency resolution, such as are found at synchrotron sources. A significant issue to be resolved for each material studied is the nature of the implanted muon site. In the case of a single muon site the analysis is straightforward, but for more complex materials, the magnetic-field distributions discussed above may be of relevance. For materials that show gaps in the spin excitation spectrum due to dimerization and singlet formation, μSR is particularly useful in measuring the temperature dependence of the spin fluctuations via the muon-spin relaxation. In conclusion, it is expected that μSR will continue to play an important role in characterizing and studying organic and molecular magnets.

This work has been supported by the EPSRC (UK). I thank F. L. Pratt, T. Sugano and M. Kurmoo for many fruitful discussions and for their contribution to this work. I am also very grateful to my other collaborators, including W. Hayes, A. Husmann, Th. Jestädt, B. W. Lovett and I. M. Marshall.

References

Allemand, P.-M., Khemani, K. C., Koch, A., Wudl, F., Holczer, K., Donovan, S., Grüner, G. & Thompson, J. D. 1991 *Science* **253**, 301.

Benoit, A., Flouquet, J., Gillon, B. & Schweizer, J. 1985 *J. Magn. Magn. Mater.* **31**–**34**, 1155.

Blundell, S. J. 1997 *Appl. Magn. Res.* **13**, 155.

Blundell, S. J., Pattenden, P. A., Valladares, R. M., Pratt, F. L., Sugano, T. & Hayes, W. 1994 *Solid St. Commun.* **92**, 569.

Blundell, S. J., Pattenden, P. A., Pratt, F. L., Valladares, R. M., Sugano, T. & Hayes, W. 1995 *Europhys. Lett.* **31**, 573.

Blundell, S. J., Sugano, T., Pattenden, P. A., Pratt, F. L., Valladares, R. M., Chow, K. H., Uekusa, H., Ohashi, Y. & Hayes, W. 1996 *J. Phys.: Condens. Matter* **8**, L1.

Blundell, S. J., Pattenden, P. A., Chow, K. H., Pratt, F. L., Sugano, T. & Hayes, W. 1997*a* *Synth. Met.* **85**, 1745.

Blundell, S. J., Pattenden, P. A., Pratt, F. L., Chow, K. H., Hayes, W. & Sugano, T. 1997*b* *Hyp. Int.* **104**, 251.

Blundell, S. J., Pratt, F. L., Pattenden, P. A., Kurmoo, M., Chow, K. H., Jestädt, T. & Hayes, W. 1997*c* *J. Phys.: Condens. Matter* **9**, L119.

Bowden, G. J. & Clark, R. G. 1981 *J. Phys.* C **14**, L827.

Brandt, E. H. 1988 *Phys. Rev.* B **37**, 2349.

Bramwell, S. T. & Holdsworth, P. C. W. 1993 *J. Phys.: Condens. Matter* **5**, L53.

Chappert, J. 1984 In *Muons and pions in materials research* (ed. J. Chappert & R. I. Grynszpan). Elsevier.

Chittipeddi, S., Cromack, K. R., Miller, J. S. & Epstein, A. J. 1987 *Phys. Rev. Lett.* **58**, 2695.

Chouteau, G. & Veyret-Jeandey, Cl. 1981 *J. Physique* **42**, 1441.

Cox, S. F. J. 1987 *J. Phys.* C **20**, 3187.

Dalmas de Réotier, P. & Yaouanc, A. 1997 *J. Phys.: Condens. Matter* **9**, 9113.

Denison, A. B., Graf, H., Kündig, W. & Meier, P. F. 1979 *Helv. Phys. Acta* **52**, 460.

Garçia-Muñoz, J. L., Cirujeda, J., Veciana, J. & Cox, S. F. J. 1998 *Chem. Phys. Lett.* **293**, 160.

Hayes, W. 1995 *Phil. Trans. R. Soc. Lond.* A **350**, 249.

Imachi, R., Ishida, T., Nogami, T., Ohira, S., Nishiyama, K. & Nagamine, K. 1997 *Chem. Lett.*, p. 233.

Kahn, O. 1993 *Molecular magnetism.* New York: VCH.

Kinoshita, M. 1994 *Japan. J. Appl. Phys.* **33**, 5718.

Kurmoo, M. & Kepert, C. J. 1998 *New J. Chem.* **22**, 1515.

Lappas, A., Prassides, K., Vavekis, K., Arcon, D., Blinc, R., Cevc, P., Amato, A., Feyerherm, R., Gygax, F. N. & Schenck, A. 1995 *Science* **267**, 1799.

Le, L. P., Keren, A., Luke, G. M., Wu, W. D., Uemura, Y. J., Tamura, M., Ishikawa, M. & Kinoshita, M. 1993*a* *Chem. Phys. Lett.* **206**, 405.

Le, L. P. (and 13 others) 1993*b* *Phys. Rev.* B **48**, 7284.

Lee, S. L., Pratt, F. L., Blundell, S. J., Aegerter, C. M., Pattenden, P. A., Chow, K. H., Forgan, E. M., Sasaki, T., Hayes, W. & Keller, H. 1997 *Phys. Rev. Lett.* **79**, 1563.

Lovett, B. W., Blundell, S. J., Jestädt, Th., Pratt, F. L., Hayes, W., Kurmoo, M. & Tagaki, S. 1999 *Synth. Met.* **103**, 2034.

McKeehan, L. W. 1933 *Phys. Rev.* **43**, 913.

Morenzoni, E., Kottmann, F., Maden, D., Matthias, B., Meyberg, M., Prokscha, T., Wutzke, T. & Zimmermann, U. 1994 *Phys. Rev. Lett.* **72**, 2793.

Mukai, K., Nishiguchi, H. & Deguchi, Y. 1967 *J. Phys. Soc. Japan* **23**, 125.

Mukai, K., Ueda, K., Ishizu, K. & Deguchi, Y. 1982 *J. Chem. Phys.* **77**, 1606.

Nagamine, K., Miyake, Y., Shimomura, K., Birrer, P., Iwasaki, M., Strasser, P. & Kuga, T. 1995 *Phys. Rev. Lett.* **74**, 4811.

Pratt, F. L., Valladares, R., Caulfield, J., Deckers, I., Singleton, J., Fisher, A. J., Hayes, W., Kurmoo, M., Day, P. & Sugano, T. 1993 *Synth. Met.* **61**, 171.

Pratt, F. L., Sasaki, T., Toyota, N. & Nagamine, K. 1995 *Phys. Rev. Lett.* **74**, 3892.

Pratt, F. L., Blundell, S. J., Hayes, W., Ishida, K., Nagamine, K. & Monkman, A. P. 1997 *Phys. Rev. Lett.* **79**, 2855.

Saint Paul, M. & Veyret, C. 1973 *Phys. Lett.* **45A**, 362.

Schenck, A. 1985 *Muon spin rotation spectroscopy.* Bristol: Adam Hilger.

Seeger, A. & Brandt, E. H. 1986 *Adv. Phys.* **35**, 189.

Sugano, T., Kurmoo, M., Day, P., Pratt, F. L., Blundell, S. J., Hayes, W., Ishikawa, M., Kinoshita, M. & Ohashi, Y. 1995 *Mol. Cryst. Liq. Cryst.* **271**, 107.

Sugano, T., Blundell, S. J., Pratt, F. L., Hayes, W., Uekusa, H., Ohashi, Y., Kurmoo, M. & Day, P. 1997 *Mol. Cryst. Liq. Cryst.* **305**, 435.

Sugano, T., Blundell, S. J., Pratt, F. L., Jestadt, T., Lovett, B. W., Hayes, W. & Day, P. 1999 *Mol. Liq. Cryst.* (In the press.)

Tamura, M., Nakazawa, Y., Shiomi, D., Nozawa, K., Hosokoshi, Y., Ishikawa, M., Takahashi, M. & Kinoshita, M. 1991 *Chem. Phys. Lett.* **186**, 401.

Uemura, Y. J., Keren, A., Le, L. P., Luke, G. M., Sternlieb, B. J. & Wu, W. D. 1994 *Hyp. Int.* **85**, 133.

Valladares, R. M., Fisher, A. J., Blundell, S. J. & Hayes, W. 1998 *J. Phys.: Condens. Matter* **10**, 10 701.

Discussion

M. Verdaguer (*Chimie des Metaux de Transition, Université Pierre et Marie Curie, Paris, France*). Some data related to high spin molecules can be added (or will be added soon) to the impressive list of muon studies on molecular magnets.

S. J. Blundell. Constraints of time did not allow me to mention these, but work on $Mn_{12}O_{12}$ acetate has been published by Lascialfari *et al.* (1998) that shows that muons are sensitive to the fluctuations in thermal equilibrium of the orientation of the magnetization. Related work has been recently performed on an Fe_8 system (Salman *et al.* 1999). Muons can therefore be used to study effects such as quantum tunnelling of magnetization in systems for which the dynamics falls in the appropriate time window.

M. Verdaguer. One of the problems with muon studies is the location of implantation of the muon. If we think that the muon is a small proton, are there evidences of 'chemical' interactions (acid–base interactions) between the muon and some specific sites of molecular crystals (perchlorates, amines), or is Dr Blundell engaged in such studies?

S. J. Blundell. In molecular systems, such interactions are indeed important and have begun to be studied. Muonium can form various muonated radicals that can be studied using level-crossing resonances. In ionic crystals, μ^+ tends to form a hydrogen bond with species such as F^- or O^{2-}. To be sensitive to local magnetism, one needs a significant fraction of muons implanted in diamagnetic states. In *p*-NPNN we observed a large diamagnetic fraction giving rise to spin precession, but we also observed a paramagnetic fraction, indicating that more than one state may be formed in a single experiment. The Oxford group are currently involved in experiments on organic molecules such as TCNQ, TTF and BEDT-TTF, which are building blocks for various organic magnets and superconductors, in order to study the nature of the implanted muon states in some detail. We are also performing similar experiments on conducting polymers and liquid crystals. In any case, for organic magnets, any uncertainty in the muon site does not prevent us from following the temperature dependence of the order parameter and studying any associated fluctuations.

Additional references

Lascialfari, A., Jang, Z. H., Borsa, F., Carretta, P. & Gatteschi, D. 1998 *Phys. Rev. Lett.* **81**, 3773.

Salman, Z., Keren, A., Mendels, P., Scuiller, A. & Verdaguer, M. 1999 *Physica*. (In the press.)